Steel and Composite Structures, *Vol. 28, No. 2 (2018) 179-194*
DOI: https://doi.org/10.12989/scs.2018.28.2.179

Assessment of dynamic crushing and energy absorption characteristics of thin-walled cylinders due to axial and oblique impact load

N. Baaskaran [*1], K. Ponappa [1] and S. Shankar [2]

[1] *Department of Mechanical Engineering, Kongu Engineering College, Erode, Tamilnadu, India*
[2] *Department of Mechatronics Engineering, Kongu Engineering College, Erode, Tamilnadu, India*

(*Received July 14, 2017, Revised April 13, 2018, Accepted May 10, 2018*)

Abstract. Reliable and accurate method of computationally aided design processes of advanced thin walled structures in automotive industries are much essential for the efficient usage of smart materials, that possess higher energy absorption in dynamic compression loading. In this paper, most versatile components i.e., thin walled crash tubes with different geometrical profiles are introduced in view of mitigating the impact of varying cross section in crash behavior and energy absorption characteristics. Apart from the geometrical parameters such as length, diameter and thickness, the non-dimensionalized parameters of average forces which control the plastic bending moment for varying thickness has explored in view of quantifying its impact on the crashworthiness of the structure. The explicit finite element code ABAQUS is utilized to conduct the numerical studies to examine the effect of parametric modifications in crash behavior and energy absorption. Also the simulation results are experimentally validated. It is evident that the circular cross-sectional tubes are preferable as high collision impact shock absorbers due to their ability in withstanding axial and oblique impact loads effectively. Furthermore, the specific energy absorption (SEA), crash force efficiency (CFE), plastic bending moment, peak force responses and its impact for optimally tailoring a design to cater the crashworthiness requirements are investigated. The primary outcome of the study is to provide sufficient information on circular tubes for the use of energy absorbers where impact oblique loading is expected.

Keywords: thin-walled structures; dynamic compression loading; energy absorption; plastic bending moment; high collision impact; crashworthiness

1. Introduction

Thin walled shell structures possess the capability of larger energy absorption and it can be widely employed in the automobile, marine, aeronautical and defense structures owing to its low structural weight corresponding to its high load bearing capacity (Huang *et al*. 2010). The objective of automobile manufacturers is to design lighter vehicles that possess high energy absorption under impact loading. The lighter materials with high ultimate strength are the basic requirement in choosing the appropriate materials. During the recent years, the attention is focused on light weight structures and crashworthiness to envisage the analytical, experimental and finite element approaches to interpret the peak force, mean force, collapse mode and energy absorption (Abramowicz and Jones 1984a, b, Hou *et al*. 2007). Crashworthiness is defined as the ability of a restraint system or component to withstand loads below a certain level and reduce the damage caused in those cases involving excessive dynamic loading. Due to the availability of various types of crashworthiness members, the thin walled structures attracted much interest among researchers because of its low cost, ease of fabrication and possessing significant energy absorbing efficiency (Mamalis *et al*. 1991, Vinayagar and Kumar 2017). The prominent features of thin walled structures involve the absorption of kinetic energy during collision through the plastic deformation (Jones 1989) and its location on sedan car as shown in Fig. 1. The foremost priority is to reduce the initial peak load on the occurrence of collapse process to improve the overall stability of structure (Alaghamdi 2001).

While the vehicle experiencing the impact scenario, the vehicular structure experiences the collapse in the combina-

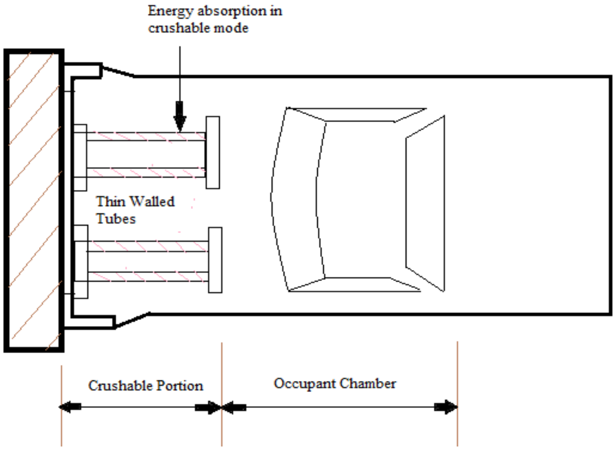

Fig. 1 Frontal linear thin walled tubes

∗Corresponding author, Assistant Professor,
E-mail: baaskararcher@kongu.ac.in
[a] Associate Professor, E-mail: kponappa@kongu.ac.in
[b] Professor, E-mail: shankar@kongu.ac.in

http://www.techno-press.org/?journal=scs&subpage=6
ISSN: 1229-9367 (Print), 1598-6233 (Online)

tion of axial and non-axial (oblique) loads rather than pure axial (or) bending loads (Abramowicz and Weirzbicki 1988). Even though the crash box design is mainly concerned in terms of axial bending modes, sufficient weight should be imposed on oblique loading in terms of CFE because it always interested in reduction of energy absorption capability of the structure. Prevailing the real case scenarios of energy absorption, the past investigations mainly focused on axial impact rather than off axis loading that can take place in the actual case (Santosa *et al*. 2000). It is indicated that the crushing response of prismatic members has increased much attention as energy absorbers in present scenarios (Han and Park 1999, Vahdatazad and Ebrahimi 2016). For example, previous work (Reyes and Langseth 2002) performed a numerical and experimental analysis on oblique loading of thin walled structures. For instance, the response of aluminum square profile tubes subjected to oblique loading has been investigated numerically and experimentally. The impact of striker angle in the crash response at the operating range of 0-30˚ in foam filled square and circular tubes have examined. The numerical results showed the energy absorption capacity has significantly reduced (Borvik *et al*. 2003) when the introduction of striker angle exceeds 15° resulting in global bending mode. The circular tube (Abramowicz and Jones 1984b) is subjected to quasi-static loading and observed an axi-symmetrical fold pattern which results in the formulation of the simple expression for the mean crushing force to validate the concept of static plastic hinge theoretical model. The axial and off-axis loading (5-35°) of conical composite tubes results in significant reduction of energy absorption pattern (Karbhari and Chaoling 2003). Till date, studies on crash response and its direct impact on energy absorption with varying thickness are not available. The salient features of the present study are to simulate the behavior of thin walled tubes subjected to both direct and oblique loading and quantify the energy absorption characteristics with respect to thickness, the angle of the striker, lengths and different perimeter of varying cross sections. Towards this end, the prioritized intention is to configure the striker angle and thickness to commence the progressive axial buckling to overall bending mode.

2. Materials and methods

The hollow structures facilitate ease in all choices of energy absorption medium due to its plastic behavior when subjected to compressive forces which are most common in structural elements. The material property, geometric configuration, impact speed, inertia of the impact mass are the significant terms mainly associated with the deformation which has a direct impact on energy absorption of thin walled tubes when subjected to dynamic loading with high velocities (Karagiozova and Jones 2004). The dual-phase steel is a high strength steel which possesses higher strength and durability, a key factor in replacing the conventional steel materials in automobile, aerospace industry and in defense sectors. The key advantage of using this material (Yu *et al*. 2009) in impact application is to enhance the energy absorption and crashworthiness in the structure.

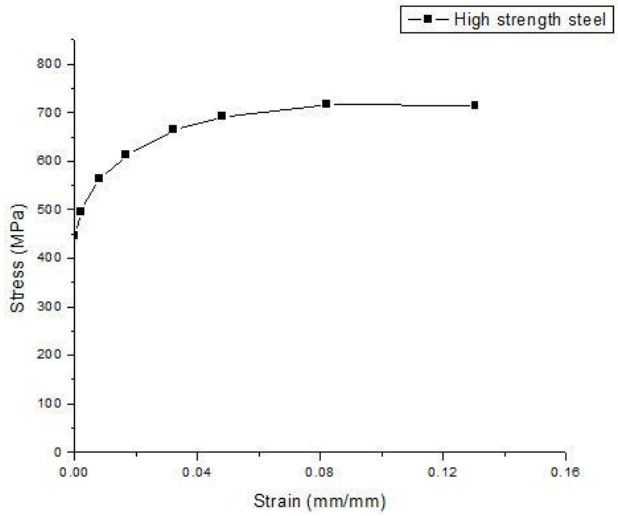

Fig. 2 Stress-strain characteristic of the steel

The high strength thin walled tubes is subjected to impact loading as per ASTM E8-04, using MTS 819N 50 kN universal testing machine with closed loop control mode to perform quasi-static tensile tests (Tai *et al*. 2010).

Fig. 2 plots the typical stress strain curve and Table 1 represents the material parameters for high strength steel. 0.2% offset method is employed to determine the corresponding yield stresses i.e., 446 MPa. The linear regression method is employed to determine the young's modulus i.e., 207. 2 GPa obtained between 0.1 σy to 0.9 σy. The Cowper-Symonds equation is employed for determining the curves for different strain rates. The strain value is calculated using stress-strain relationship during the dynamic loading of thin walled structures (Peixinho and Pinho 2007), the change observed in strain value is to be inversely proportional. Numerous investigations have been carried out on constitutive laws relating the influence of strain rate on material properties (Duffy 1979). To formulate the stress-strain behavior from the obtained dynamic load the regression formula is introduced, the corresponding dynamic yield stress can be calculated using the Eq. (1) from the static strength

Table 1 Material parameters for high strength steel

High strength steel	Density (kg/m^3)			E (GPa)			SIGY (MPa)	
	7820			207.2			446	
Stress (MPa)	446.0	496.6	563.1	612.7	664.2	691.5	717.8	714.4
Strain (mm/mm)	0.0	0.00183	0.00805	0.01678	0.0321	0.0481	0.0819	0.1304

$$\dot{\epsilon} = D\left(\frac{\sigma_{dy}}{\sigma_y} - 1\right)^n$$

$$\sigma_{dy} > \sigma_y \qquad (1)$$

$$\sigma_{dy} = \sigma_y \left(1 + \left|\frac{\dot{\epsilon}}{D}\right|\right)^{1/n}$$

3. Performance indicators in measurement of energy absorption

Under the crash response, the following parameters are accounted and it plays the crucial role in determining the energy absorption (E_a), Peak Force (F_{MAX}) and Crash force efficiency (CFE). When the thin-walled structures subjected to quasistatic loading, it reaches the maximum load before the start of deformation. This force experienced by the structure called as the peak force (F_{MAX}) and it is the main factor for breaking the initial stiffness of the structure. The mean load is defined as the force required for the formation of folds in a structure (Langseth and Hopperstad 1996) which is governed by the Eq. (2).

$$P_m = \frac{E_a}{\Delta} \qquad (2)$$

E_a - Absorbed energy, Δ - Displacement

The total energy absorbed (Chung *et al*. 2008) can be calculated work done by crushing force (F) on a longitudinal displacement (Δ) by the following Eq. (3).

$$E_a = \int_0^{\Delta} F.d\Delta \qquad (3)$$

The area below the curve of load vs. displacement can be obtained by the trapezoidal rule and it can be obtained by rewriting the Eq. (4) which gives the (E_a) and is defined as (Thornton *et al*. 1983)

$$E_a = \frac{1}{2}\sum_{i}^{n-1}(F(\Delta)_{i+1} + F(\Delta)_i).((\Delta)_{i+1} - (\Delta)_i) \qquad (4)$$

The energetic efficiency can be determined by plotting the relationship between absorbed energy (E_a), peak force (F_{MAX}) and displacement (Δ). The specific energy absorption (SEA) is defined (Krauss and Laananen 1994) as the ratio between the energy absorbed (E_a) to the mass of the thin walled member.

$$SEA = \frac{E_a}{M} \qquad (5)$$

The crush force efficiency (Tarlochan and Samer 2013) is defined as the ratio between the mean crushing forces (P_{mean}) to the maximum crushing force (P_{max}).

$$CFE = \frac{P_{mean}}{P_{max}} \qquad (6)$$

4. Numerical analysis

4.1 Finite element modelling

The general geometry and FEM model of the thin walled structure tubes were analyzed in this study as shown in Fig. 3. A non-linear FE code ABAQUS-Explicit was used to carry out the numerical simulations of dynamic compression of thin-walled tubes under impact loading. In the present phase, five different thin walled structural cross-sectional profiles include circle, square, rectangle, hexagon and octagon was investigated. The high strength steel of

Table 2 Geometry and dimensions of thin walled tubes used for study

Description	Specimen ID	Perimeter (mm)	Length (mm)	Major dimension (mm)	Thickness (mm)	Profile
Circular	C/300 C/372	300 372	350	Diam.= 95.5 Diam.= 118.1	2,2.5,3	
Rectangle	R/300 R/372	300 372	350	90X60 112X74	2,2.5,3	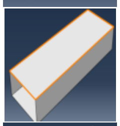
Square	R/300 R/372	300 372	350	75X75 93X93	2,2.5,3	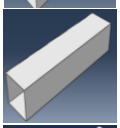
Hexagonal	H/300 H/372	300 372	350	50 62	2,2.5,3	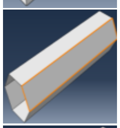
Octagonal	O/300 O/372	300 372	350	37.5 46.5	2,2.5,3	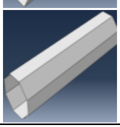

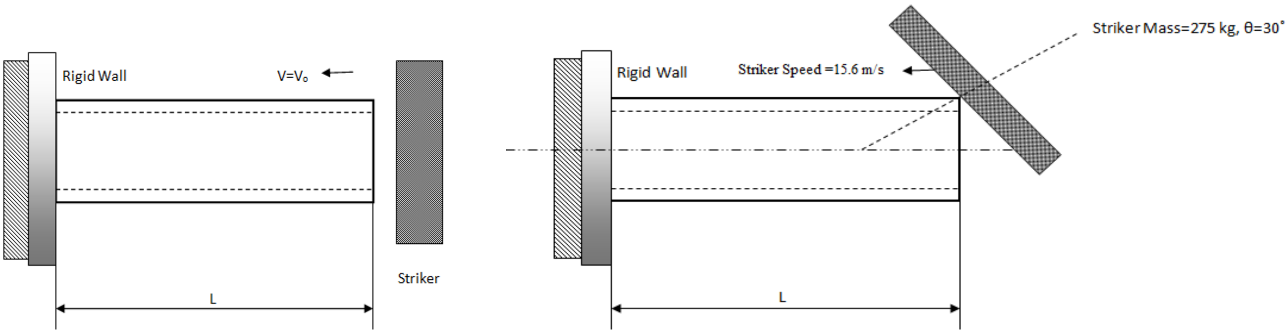

Fig. 3 Exhibits the schematic geometrical setup of circular tubes subjected to direct and oblique loading with uniform thickness (t) and Length (L)

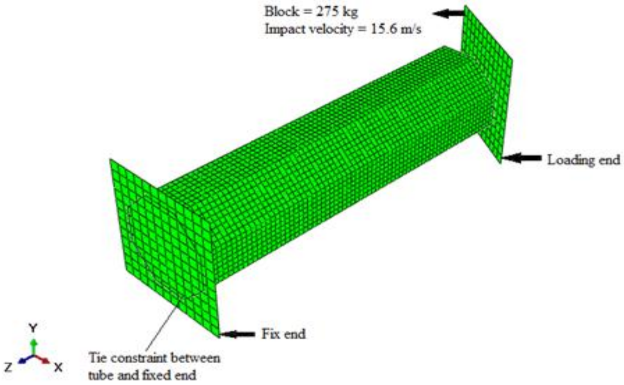

Fig. 4 Discrete model and Boundary condition

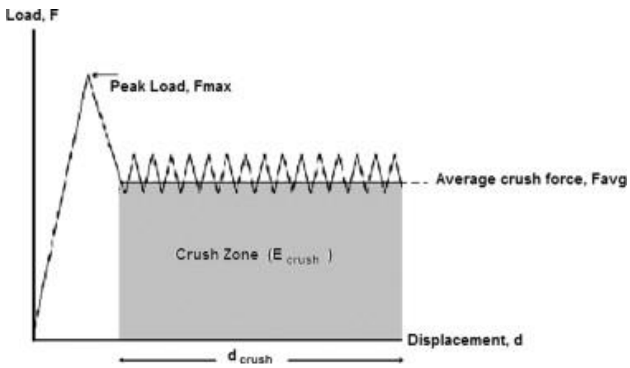

Fig. 5 A typical Force Vs. Displacement of axial crushing of circular tubes (32)

various sections of length and thickness 350 mm and 2 mm were considered. The two sets were chosen for the above cross sectional parameters, namely 300 mm and 372 mm for all profiles of the tube. The particulars about the design of experiments to be simulated are shown in Table 2. A schematic diagram of the finite element model coupled with boundary and loading conditions of the tubular members with an impactor is shown in Fig. 4. The average perimeter is normally chosen based on the study on sedan and compact cars available in the market (Qi *et al*. 2012). The impact cases carried out for two different loading patterns which include direct and oblique loading of 30° off the thin walled longitudinal axis. However, research information on

Table 3 Comparison of the absorbed energy and peak crushing force values obtained from finite element model of the present study to those obtained from Tarlochan *et al*. (2013)

Descriptions	P_{max} (kN)	Energy (kJ)
(A) Finite element results (Tarlochan *et al*. 2013)	243.53	24.49
(B) Finite element result of the present study	232.47	25.82
% Difference between B and A	-4.75	5.15

the oblique loading of thin-walled structures at an offset of 30° was chosen due to the maximum load enhancement without compromising the mean force (Ahmad and Thambiratnam 2009). The typical axial crashing force and displacement for an explicit impact model was shown in Fig. 5.

4.2 Validation of the numerical model

To investigate the energy absorption of thin walled structures, relevant experimental or FEA experiments must be performed to validate the force-displacement curves, energy absorption and collapse modes to pinpoint the modeling accuracy. The crashing force versus displacement relationship, collapse modes and energy absorption obtained from the present work were compared with the previous case (Tarlochan and Samer 2013).

The material was modeled using the A36 steel (mild steel) and geometric parameters of length 350 mm, thickness and diameter 100 mm was considered. The typical force-displacement characteristics and energy absorption of type C/372 was compared in Table 3, it shows the energy absorption and peak force of 25.82 kJ and 232.47 kN (present results) when compared to 24.49 kJ and 243.53 kN for our predecessor and the relative error of 6% was obtained which was acceptable in actual engineering cases. The obtained force-displacement curve looks much similar and shown in Fig. 6. The good agreement between both analyses was observed, which enable us with the confidence to evaluate the energy absorption, collapse modes with the sufficient accuracy.

Table 4 The material parameters

	Johnson-Cook material parameters					Cowper-symonds parameters				
Material	Density (Kg/m^3)	*A* (Mpa)	*B* (Mpa)	C_p (J/Kg K)	T_{melt} (K)	*n*	*c*	*m*	$C(S^{-1})$	*P*
Al 2024	2770	265	426	875	775	0.34	0.015	1.0	6500	4

* T_{melt} = melting temperature; $C_P = Sp$. Heat capacity; *A*, *B*, *n*, *c*, *m*, *C* and *P* are material constants

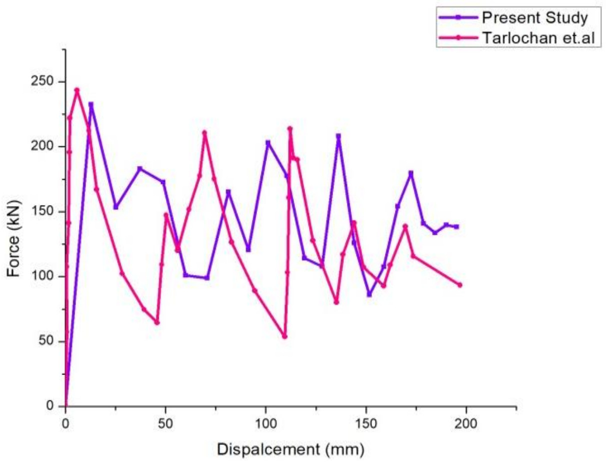

Fig. 6 Force Vs. Displacement of circular tubes

Fig. 8 Experimental set-up (type-DEEPAK (DTRX))

4.3 Experimental validation

To validate the developed FE model, axial crushing test on simple and patterned tubes along with elliptical holes was conducted as shown in Fig. 7. The tubes were of circular cross sections of aluminium 2024 alloy, with length being 128 mm, diameter being 52 mm and wall thickness being 0.0072 mm. There were three holes on the outer peripheral area in which the line of axis of each hole was maintained in the straight line. The holes were positioned at equal distance on the surface of the wall, having the different configurations maintaining the cross-sectional area of 78.53 mm^2. The elapsed distance between the centre of the top (bottom) and the top (bottom) of the tube was 32 mm. The linear distance between the lines of axis to the left or right exterior end of the tube was set as 26 mm.

The material parameters considered were as follows: Young's modulus E = 69000 MPa and Poisson's ratio ν = 0.35, plasticity models are given in the Table 4. The test was performed on a universal testing machine (type-DEEPAK (DTRX)). The specimen along with the mounting fixture was placed freely on the bottom disc and the crushing of the tube was performed by the downward movement of top disc. In this course, it was opted to choose 5 mm/min to ensure the performed tests were within quasi-static range. The crushing loads and displacements were

Fig. 7 Simple tube fixed on mounting fixture

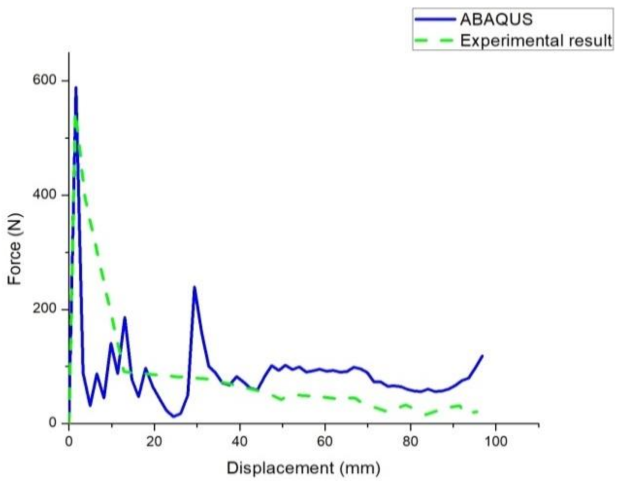

Fig. 9 *F-D* curve of simple tube

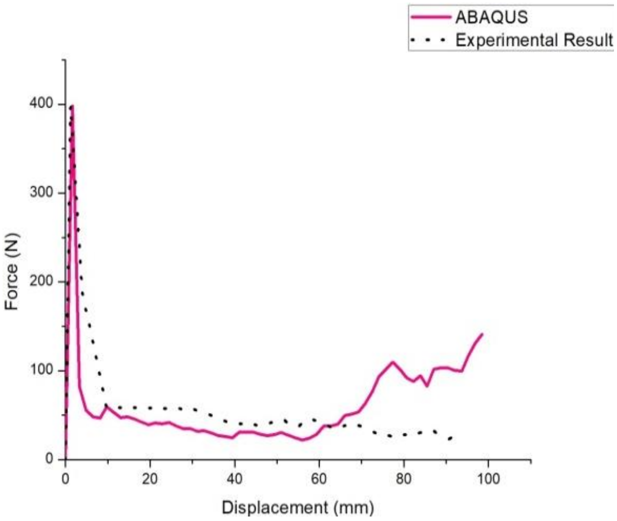

Fig. 10 F-D curve of Patterned tube (Elliptical holes)

captured by an in-built automatic data acquisition system. The force- displacement curves of simple and patterned tubes was shown in Figs. 9 and 10 for both experimental and numerical simulations. The numerical simulations was initially run with θ = 0° for quasi-static loading pattern using ABAQUS, formulating the similar boundary condition and contact of the tube were as same as that to be followed in experiments. It can be noted that the force-displacement pattern of experiment coincides well with that of simulation for both simple and patterned tubes. Comparing the above for both energy absorption (E_a) and peak force ($P_{\max}$), the variation of results between experimental and simulations results for each tube was within 10%, as shown in Table 5. Fig. 11 represents the collapse pattern (Experimental and Numerical) for elliptical patterned tubes, in which the deformed shapes, collapse mode (Diamond) and collapse starting point was similar.

The developed FE model presented good coincidence in predicting the force- displacement curves and collapse pattern for both simple and patterned tubes which was subjected to quasi-static loading, which assure the noteworthiness of crash force indicators extracted for the different cross-section profiles subjected to impact loading.

4.4 Numerical simulation

In the present study, finite element (FE) models and simulations were developed using the nonlinear FE code ABAQUS-EXPLICIT in view of obtaining the accurate and realistic results. The main concern was to predict the crash response of the thin walled structures when subjected to the impact mass. The complete model consists of thin walled tubes subjected to the rigid wall in bottom and striker or base at the top loading end with direct or 30° oblique impact. Fig. 2 plots the typical stress strain curve and Table 1 represents the material parameters for high strength steel which was used to model the thin-walled member. All the tubes were modeled using 4 node shell continuum (S4R) elements comprising of 5 integration points along the thickness direction of the element. The striker was modeled using R3D4 elements, possesses only one allowable translational displacement in impact direction, remaining other degrees of freedom were constrained and modeled as whole rigid body. The mesh convergence study was performed to ensure a required mesh density to capture the crushing process. Based on the mesh convergence study, the local seeds of approximate element size of 5 mm for a total of 4200 quadrilateral dominated element were used for free meshing. The general contact algorithm was used to simulate the contact interaction between the components to eliminate the interpenetration of thin-walled structures with the striker and rigid wall and also possess the advantage of less computational time. The contacts between the thin-

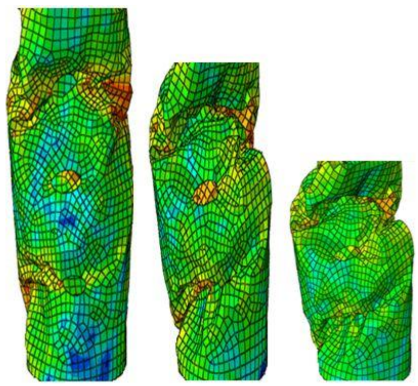

Fig. 11 Collapse pattern for elliptical patterned tubes (Experimental and Numerical)

Table 5 Numerical and experimental values of peak force and energy absorption of simple and patterned tubes

Specimens	$P_{\max}$(N) Num./Expt.	% Difference	Energy (J) Num./Expt.	% Difference
Simple	588.88/547.10	7.09	8.351/7.940	4.92
Elliptic	398.18/399.25	-0.26	5.729/5.235	7.05

walled structure and striker were modeled as contact algorithm based on a finite sliding penalty with contact pairs and hard contact. The phenomenon of volumetric locking was avoided using enhancement based hourglass control to avoid the artificial zero energy deformation modes and reduced integration. The coulomb friction coefficient of 0.2 was set for all contact surfaces (Tarlochan *et al*. 2013, Baaskaran *et al*. 2017). The impact mass of 275 kg with a velocity of 15.6 m/s (56 km/h) were employed on striker to get collided with thin walled member. The NCAP (New car assessment program) by the NHTSA (National Highway Traffic safety Administration) gives the impact speed value and impact mass was assumed 25% of a compact sedan (1100 kg). In service the maximum energy absorption was less than 50% by two tubes, assuming that the thin walled structure can absorb equivalent kinetic energy of 275 kg (Witteman 1999).

5. Results and discussion

A concise brief of the results obtained in this study was shown in Tables 6 and 7. The elaborate dissertations and interpretations will be given in the upcoming sub sections.

5.1 Force-displacement behaviour of various geometric profiles

The chosen profiles were subjected to axial and oblique loading and its force-displacement diagrams were depicted in Fig. 12. The typical displacement represents the movement of the rigid striker, the joints of the striker and tube were assumed as the full contact while tube approaches crushing. Fig. 12 expresses the typical force-displacement characteristics for various cross-sectional profiles of perimeters (P-370) and (P-372) exposed to direct and oblique loading.

5.2 Effect of load angle and wall thickness

The energy absorption and dynamic response of thin-walled tubes was initially set to the standard (direct loading) of uniform thickness compared with the striker angle θ = 30° using a shell tube geometry with L = 350 mm, t = (2, 2.5, 3 mm) and an impact velocity of 15.6 m/s, which is normally encountered in crash (or) impact applications.

Fig. 7 shows a significant influence of impact angle on the force-displacement curve and peak load at initial conditions. The thin-walled tubes under direct loading with no inclination exhibit maximum initial peak load at the inception of progressive crushing followed by oscillating force and end shortening characteristics with respect to the corresponding patterned folding. However, an increase in load angle causes the reduction in load carrying capacity which directly impacts on energy absorption characteristics. The energy absorbing capacity was greatly influenced by the load angle, if the impactor profile falls away from the structure's central axis apart forms a global bending mode

Table 6 Characteristics of crashworthiness parameters for all tube profiles for two different parameters (direct loading)

Indicators	Circular		Square		Rectangle		Hexagon		Octagon	
	C/300	C/372	S/300	S/372	R/300	R/372	H/300	H/372	O/300	O/372
Thickness (t) = 2 mm										
Energy (kJ)	29.79	29.14	30.55	30.51	30.56	29.83	29.61	29.97	29.58	30.38
P_{max} (kN)	349.27	423.29	168.82	206.66	135.27	173.32	185.51	234.46	187.51	287.34
$F_{average}$e (kN)	156.91	180.33	119.32	117.37	135.61	121.88	132.74	147.06	145.55	150.32
CFE	0.44	0.42	0.70	0.56	0.98	0.70	0.71	0.62	0.77	0.32
SEA (kJ/kg)	18.61	18.21	19.09	19.06	19.10	18.64	18.50	18.73	18.48	18.98
Thickness (t) = 2.5 mm										
Energy (kJ)	27.82	28.18	29.05	25.09	28.96	28.92	29.49	28.02	29.47	28.30
P_{max} (kN)	325.15	359.58	226.53	268.65	226.52	251.32	312.51	332.24	305.12	363.80
$F_{average}$e (kN)	203.49	212.46	154.45	183.23	125.41	136.77	195.13	205.38	187.95	213.95
CFE	0.62	0.59	0.68	0.68	0.55	0.54	0.62	0.61	0.61	0.58
SEA (kJ/kg)	17.38	17.61	18.15	15.68	18.1	18.07	18.43	17.51	18.41	17.68
Thickness (t) = 3 mm										
Energy (kJ)	26.99	23.13	27.84	27.49	27.92	27.62	27.37	27.67	28.28	26.96
P_{max} (kN)	398.02	481.28	289.90	382.74	270.94	307.45	390.17	451.78	421.30	411.29
$F_{average}$e (kN)	250.38	308.09	216.99	266.07	199.49	204.46	251.73	285.96	251.05	300.94
CFE	0.63	0.64	0.74	0.69	0.73	0.66	0.64	0.63	0.59	0.73
SEA (kJ/kg)	16.86	14.49	17.4	17.18	17.45	17.26	17.10	17.29	17.67	16.85

*a P_{max} herein indicates the initial peak crashing force
*b CFE indicates the crash force efficiency
*c SEA indicates the specific energy absorption

Table 7 Characteristics of crashworthiness parameters for all tube profiles for two different parameters (oblique loading)

Indicators	Circular		Square		Rectangle		Hexagon		Octagon	
	C/300	C/372	S/300	S/372	R/300	R/372	H/300	H/372	O/300	O/372
Thickness (t) = 2 mm										
Energy (kJ)	13.75	32.57	01.43	13.57	10.15	32.49	01.40	16.66	02.31	08.58
P_{max} (kN)	104.68	202.07	57.22	131.00	99.39	127.54	111.20	127.93	63.50	101.59
$F_{average}$e (kN)	40.94	152.65	33.93	41.47	28.79	121.25	39.82	47.23	09.56	25.84
CFE	0.39	0.75	0.59	0.31	0.28	0.95	0.35	0.36	0.15	0.25
SEA (kJ/kg)	8.59	20.35	0.893	8.48	6.34	20.30	0.875	10.41	1.44	5.36
Thickness (t) = 2.5 mm										
Energy (kJ)	20.07	33.22	06.85	20.10	15.43	23.82	01.81	32.42	04.39	10.26
P_{max} (kN)	150.24	248.81	64.86	188.92	149.90	152.62	130.10	170.13	101.72	133.00
$F_{average}$e (kN)	61.96	185.58	37.64	61.18	42.89	64.12	08.68	91.30	0.411	30.85
CFE	0.41	0.74	0.58	0.32	0.28	0.42	0.06	0.53	0.40	0.23
SEA (kJ/kg)	12.54	20.76	4.28	12.56	9.64	14.88	1.13	20.26	2.74	6.41
Thickness (t) = 3 mm										
Energy (kJ)	29.75	33.06	12.36	01.27	13.07	25.13	05.27	10.88	05.50	13.45
P_{max} (kN)	296.54	272.25	77.86	133.50	165.11	189.84	152.21	128.05	117.83	240.30
$F_{average}$e (kN)	212.79	98.84	41.66	52.43	37.27	64.48	17.23	32.01	17.36	39.30
CFE	0.71	0.36	0.53	0.39	0.22	0.33	0.11	0.24	0.14	0.16
SEA (kJ/kg)	18.59	20.66	7.72	0.793	8.16	15.70	3.29	6.8	3.44	8.40

results reduction in peak load carrying capacity on contrary with thickness which was observed (Nagel and Thambiratnam 2005) in former studies on tapered rectangular tubes.

The dynamic loading caused by the impactor on thin-walled member and the corresponding deformation was disassociated with each other which clearly indicates the stiffness of the member and impactor mass were independent of each other. The deformation of the thin-walled member caused by the impact of the striker was much similar with nonlinear spring experienced in the rectangular thin- walled component under impact (Langseth *et al*. 1998).

The energy absorbed by the thin-walled tubes was represented by the area under the curve in the *F-D* diagram and Fig. 12 clearly indicates the energy absorbed in direct loading which was comparatively lower than the oblique loading. As a result of progressive crushing which leads to axial and bending of tubes subjected to oblique loading and the evident clearly reveals the *F-D* pattern was much similar for both the parameters subjected to axial and oblique loading in the tubes. To clarify the obtained results of the various comparative pattern clearly depicts the contact force and displacement under various thickness (2, 2.5, 3 mm), and the interaction between the impactor force and displacement of the member. The contribution of thickness in the parametric study clearly indicates that the displacement of the tube was approximately dependent on neither the thickness nor the impact mass of striker. The foremost priority to mitigate the impact of crash force efficiency (CFE), which facilitate the designer to choose the material as energy absorber (Nagel and Thambiratnam 2006).

The significant fact (Tarlochan and Samer 2013) lies behind the selection of crash tube can be disclosed, the derived value of CFE in case of ideal crash tube should be unity to the corresponding force displacement characteristics. The reduction in maximum peak value (CFE results) leads to maximum contribution, sudden acceleration rise creates catastrophic damage results in the maximum frontal collision which must be avoided. The CFE of 0.98 was obtained in the case of rectangular tubes of P-300 and t = 2 mm, drastic reduction of 0.55 of same P-300 at t = 2.5 mm which decreased in 56.12%. To understand further, the effect of increasing thickness t = 3 mm shows a slight increase in CFE, but it was less than its predecessors. With respect to the effect of thickness and Pmax on CFE was clearly discussed in the above section with the aid of the Tables 6 and 7. It clearly reveals that the best profile possessing high CFE, which was much desirable and it can be maximized by decreasing its peak load. The structural effectiveness was related to CFE and much essential to quantify the effectiveness of crash tube (Fyllingen *et al*. 2010).

5.3 Energy absorption characteristics

Normally, there were many factors used to access the energy absorbing behaviour of crash structures which includes average crush force ($F_{average}$), peak force (P_{max}), energy absorbed (EA) and crash force efficiency (CFE) as indexed in Tables 6 and 7 (Nagel and Thambiratnam 2005).

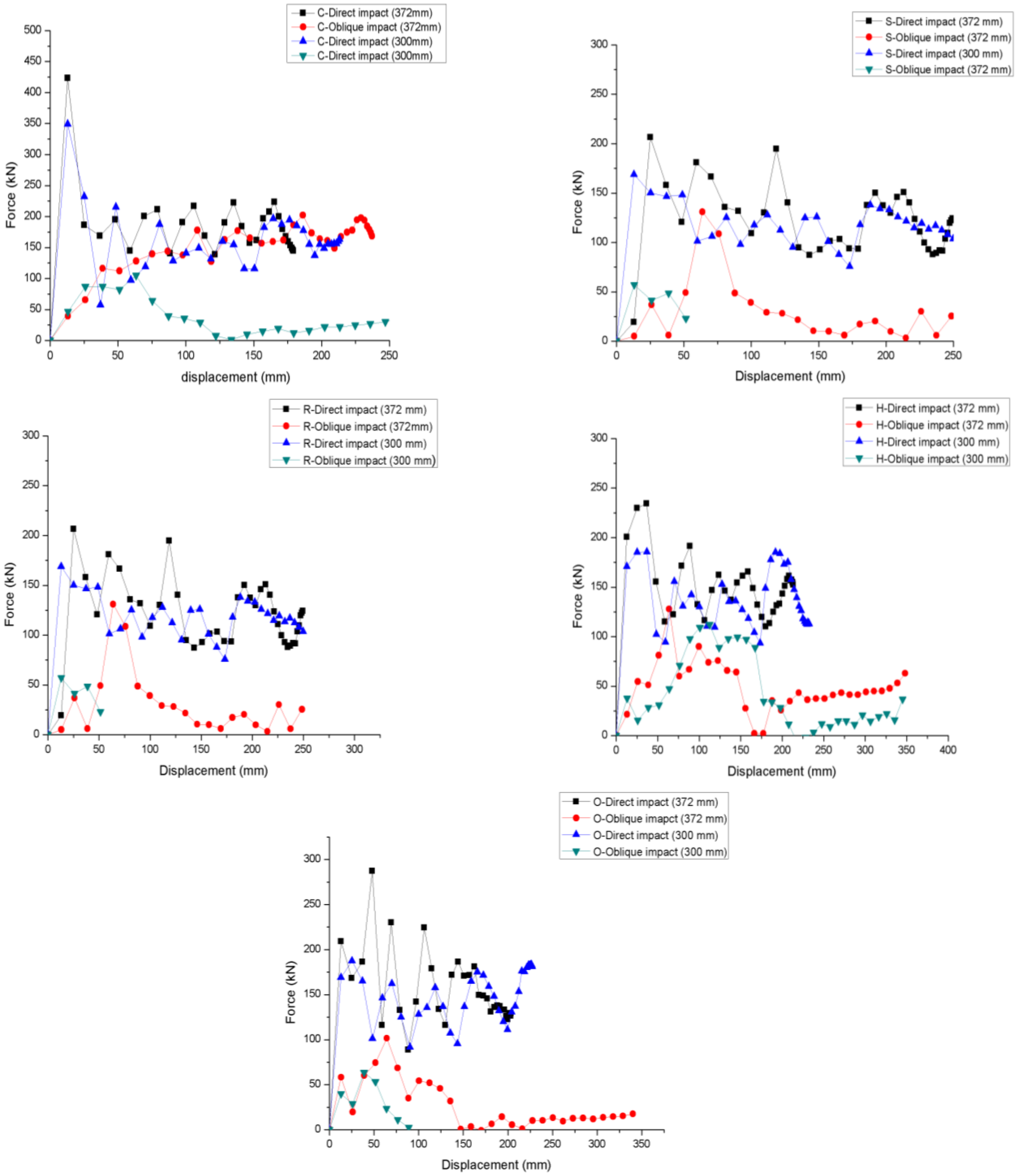

Fig. 12 Force Vs. displacement for various geometric profiles at t = 2 mm (direct and oblique impacts)

The effective destruction over the entire length of structure due to mass specific energy absorption can be expressed in terms of energy absorbing capacity (Fyllingen *et al*. 2010) and described in the following Eq. (7).

$$E_s = \frac{E_{total}}{\Delta M} = \frac{E}{A \Delta L \rho} \tag{7}$$

Where E_{total} represents the total energy absorbed whereas ΔM is the mass of the crushed thin walled structures, A is the cross sectional area and ρ is density. The different structural design concepts were compared in terms of energy absorption by means of plotting the total energy absorbed was devised neither as a function of deformation length nor as time. From the above positioned Fig. 13, it can be concluded that the lower energy absorption that can be occurred for rectangle cross section in the case of direct loading for both (P-370 and P-372) profiles invariable to its thickness parameter.

When comparing all the profiles of various thickness, the square, circular and rectangular profiles shows good comparative performance in terms of energy absorption invariably for both the cases in oblique and direct loading.

The empirical relation proposed (Guillow *et al*. 2001)

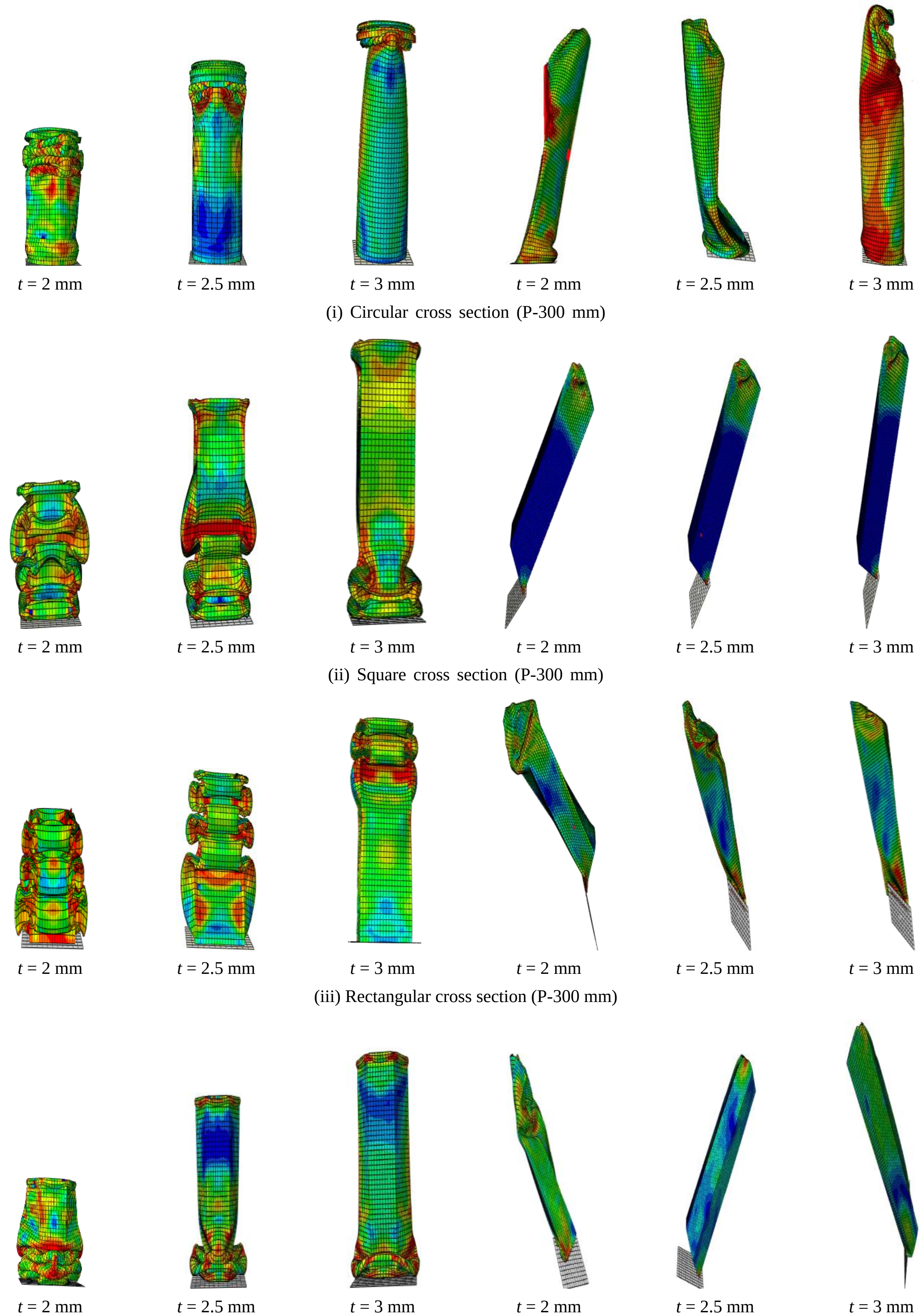

(iv) Hexagonal cross section (P-372 mm)

Fig. 13 Crashed high strength steel members of different cross sections subjected to direct and oblique loading

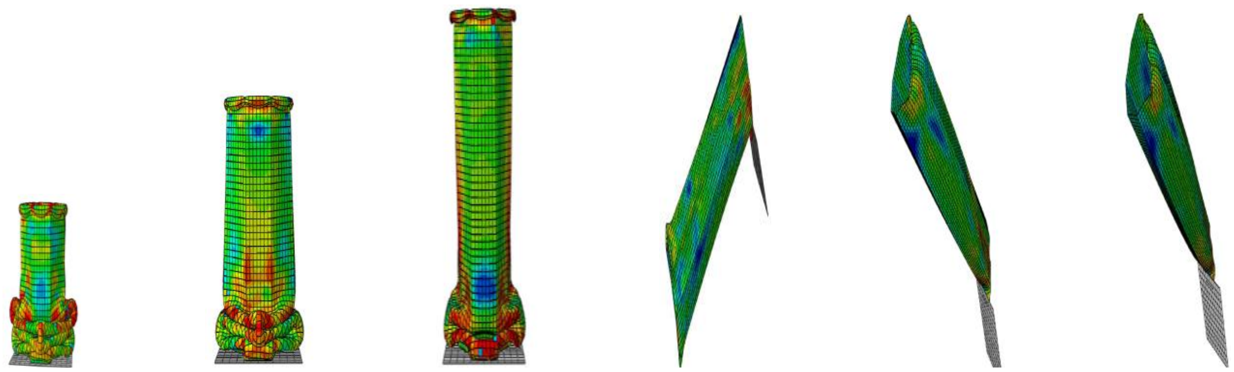

t = 2 mm t = 2.5 mm t = 3 mm t = 2 mm t = 2.5 mm t = 3 mm

(v) Octagonal cross section (P-372 mm)

Fig. 13 Continued

for axisymmetric folds to the circular tube, average crush force (Faverage) is given by the Eq. (8).

$$F_{av} = \left[72.3.\left(\frac{D}{t}\right)^{0.32}\right].\frac{\sigma_0.t^2}{4} \quad (8)$$

While considering the present scenario, for substituting the average flow stress can be given by using the empirical relation (9).

$$\sigma_0 = \frac{\sigma_{0.2} + \sigma_u}{2} \quad (1)$$

Table 8 Numerical and analytical values of average force for circular specimen subjected to direct and oblique loading

Specimen ID / loading pattern	$F_{average}$e (kN) (Numerical)	$F_{average}$e (kN) (Analytical)	% Difference
(C/300) / Direct	156.91	144.77	7.73
(C/372) / Oblique	152.65	154.91	1.47

The average crushing forces was defined as the average value of force incurred in the entire crash cycle. The circular profile exhibits significant average crushing force when compared with all other profiles. The average crush force for the present case was obtained by substituting the values in Eq. (8) for the following profiles. The circular tube of specimen ID (C/300) were subjected to direct loading and (C/372) subjected to oblique loading of the thickness (t = 2 mm) was chosen to compare with the analytic form. It shows good correlation of results between the analytical equation and FE results. The error percentage falls about 10 % which was exhibited in Table 8 provokes the obtained results were validated in terms of performance indicators. From the above study, it was evident that the energy absorption capability varies for different types of profiles which were normally calculated from the area displaced under the curve. In Fig. 14, the energy absorption was plotted as a function of the displacement of crash tubes relatively than the function of time due its capability of correlating various concepts in design.

The significance was not only providing overall energy absorption, it also enables the designer to identify the

Table 9 Energy absorption of various profiles with different loading conditions and thickness

Profile	Energy absorption (kJ)											
	Perimeter 300 mm						Perimeter 372 mm					
	Direct impact			Oblique impact			Direct impact			Oblique impact		
Thickness (t) (mm)	2	2.5	3	2	2.5	3	2	2.5	3	2	2.5	3
Circular	29.7	27.8	13.7	13.7	20.0	29.7	29.1	28.1	23.2	32.5	33.2	33.0
EA (%)				-53.8	-27.8	09.2				10.5	15.1	29.8
Square	30.5	29.0	27.8	01.4	06.8	12.3	30.5	25.0	27.4	13.5	20.1	01.2
EA (%)				-95.2	-76.4	-55.6				-55.5	-80.1	-95.3
Rectangle	30.5	28.9	27.9	10.1	15.4	13.0	29.8	28.9	27.6	32.4	23.8	25.1
EA (%)				-66.7	-46.7	-53.1				08.9	-17.6	-09.0
Hexagon	29.6	29.4	27.3	01.4	01.8	05.2	29.9	28.0	27.6	16.6	32.4	10.8
EA (%)				-95.2	-93.9	-80.7				-44.4	15.7	-60.6
Octagon	29.5	29.4	28.2	02.3	04.3	05.5	30.3	28.3	26.9	08.5	10.2	13.4
EA (%)				-92.2	-85.1	-80.5				-71.7	-63.5	-50.1

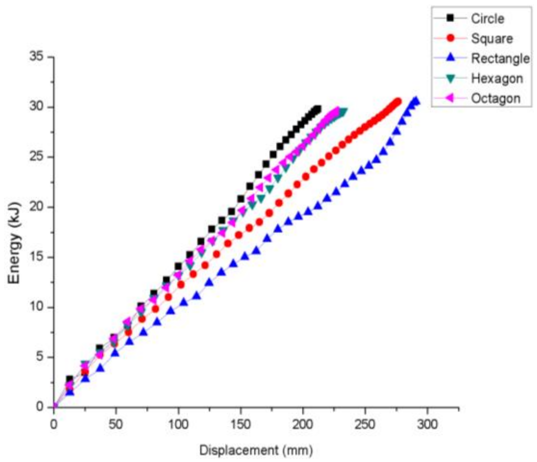

(a) Direct P-300 mm at t = 2 mm

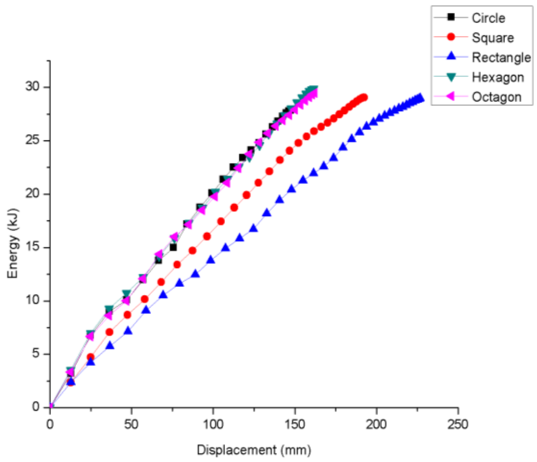

(b) Direct P-300 mm at t = 2.5 mm

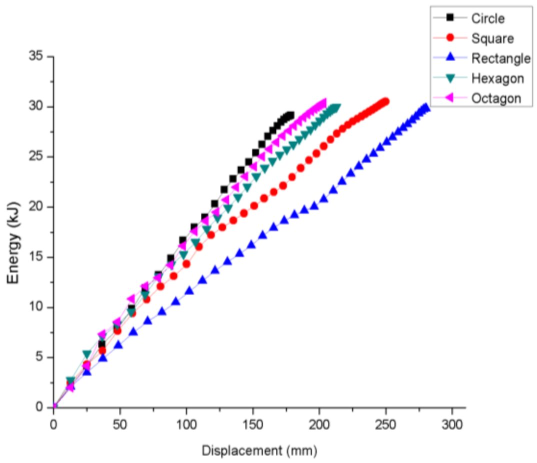

(c) Direct P-372 mm at t = 2 mm

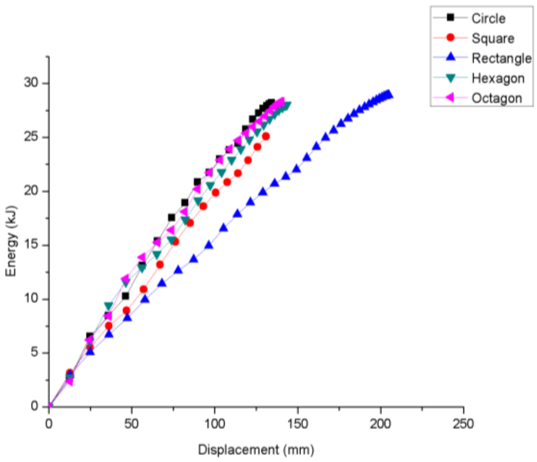

(d) Direct P-372 mm at t = 2.5 mm

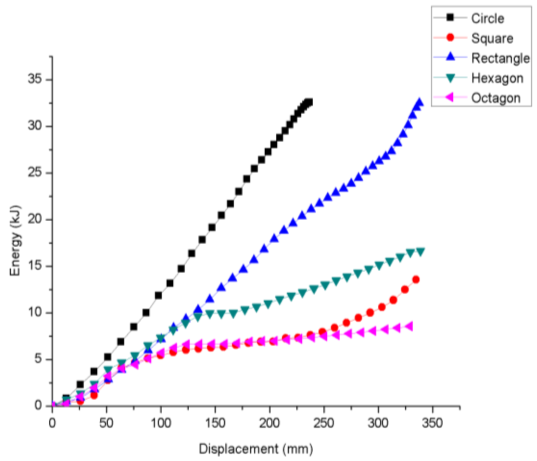

(e) Oblique P-372 mm at t = 2 mm

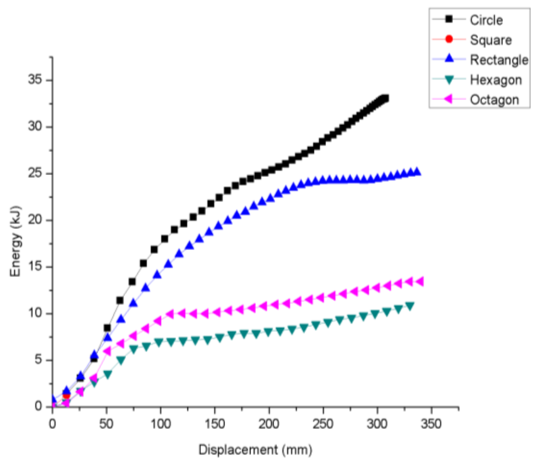

(f) Oblique P-372 mm at t = 3 mm

Fig. 14 Energy absorption characteristics of six different profiles for direct and oblique impact loading with perim eter 300 mm and 372 mm

energy absorption pattern for the corresponding displacement. Table 9 clearly reveals 80% simulation trails depicted the square cross sectional profile had convincing minimum energy absorption (EA) while compared to other profiles subjected to both direct and oblique loading. To understand further on overall energy absorption, indeed the square profile shows consistent energy absorption in direct loading than hexagonal and octagonal profile. The reason behind in picking the square profile, it provides considerable reduction in energy absorption in oblique loading than direct loading. This conclusion was supported using Table 9, it clearly reveals in both cases, reduction of energy absorption was about 95% in oblique loading as their predecessors in direct loading of P-300 and P-372. The

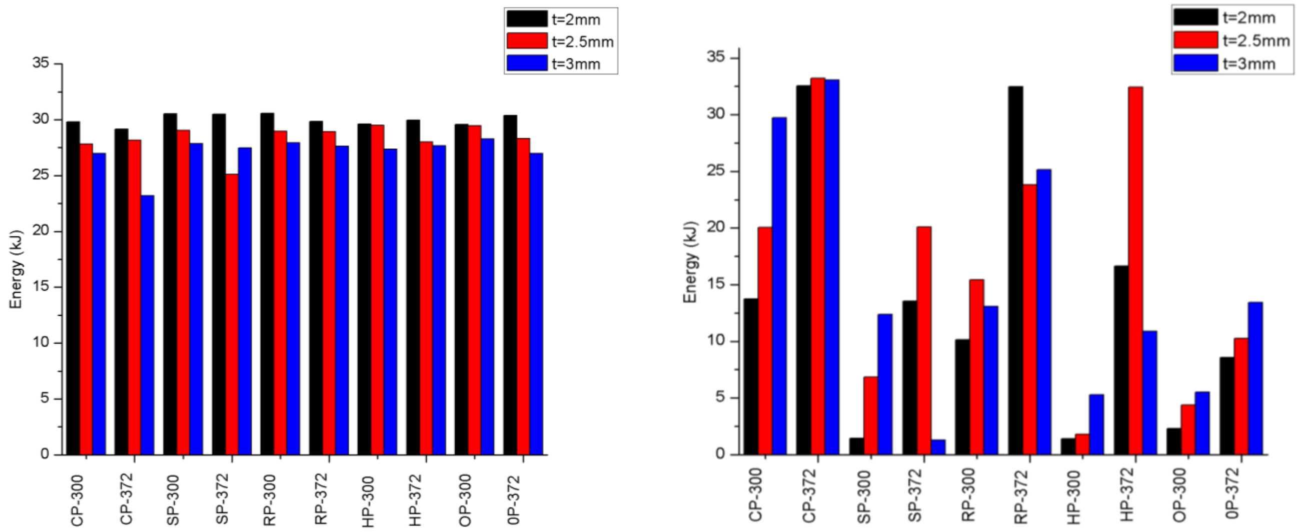

(a) Direct loading (b) Oblique loading

Fig. 15 Energy absorption characteristics of five different profiles for direct and oblique impact loading with perimeter 300 mm and 372 mm

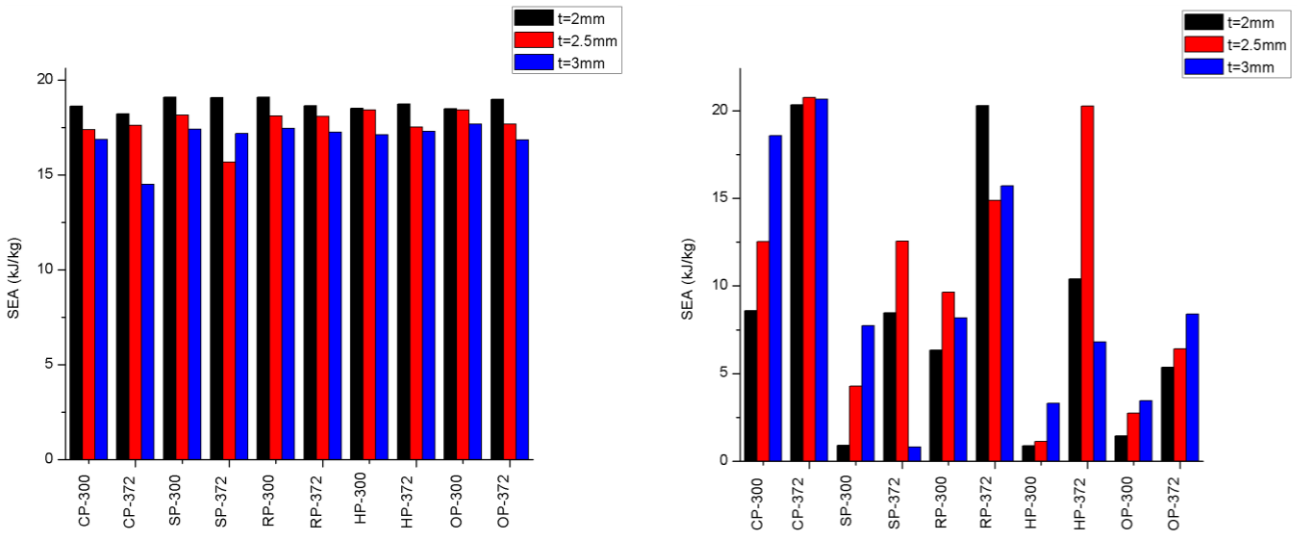

(a) Direct loading (b) Oblique loading

Fig. 16 Specific energy absorption characteristics of five different profiles for direct and

study clearly shows that, increase in a number of sides of having same perimeter experiences different energy absorbing pattern due to local buckling. Indeed the rectangular cross section provides the significant energy absorption that can be depicted in Table 5. The macro investigation reveals that the energy absorption rate was much lesser to the corresponding deflection when compared to all profiles, it indirectly indicates that the rectangular profiles undergoes maximum deformation and undergoes progressive crushing. Even though lesser energy absorption rate to the corresponding deformation was noticed, probably due to the progressive crushing results in maximum deformation, in turn, the overall energy absorption rate increases when compared with all other profiles. This phenomenon was briefly revealed in Fig. 14, where the rectangular cross section experiences a maximum displacement when subjected to both direct and oblique loading.

The octagonal and hexagonal profiles experiences lower displacement during oblique loading due to the influence of increasing turns in the profile. Probably it makes the profile to be deflected from the longitudinal axis which reduces the contact between the impactor (or) striker. To mitigate the above case which was clearly visible in Figs. 13 and 15 i.e., the energy absorption with respect to deflection was much lesser than the conventional profiles.

Inspite of comparing specific energy absorption (SEA), the square tube of perimeter 300 mm (P-300) possessed the large magnitude of SEA of 19.09 kJ/kg in direct loading for the nominal thickness of 2 mm. Contrary, in the case of oblique loading, the circular tube exhibited higher SEA of 20.35 kJ/kg for the nominal thickness of 2.5 mm subjected to P-372. The observed Figs. 15 and 16, also reveals that there was a significant change in energy absorbing pattern for oblique loading for both the perimeters. From the above observation, it clearly indicates that the energy absorption pattern which varies and decreases drastically with the oblique loading when compared to the contrary in direct loading. The formation of lobes due to progressive crushing push the tube away from the central axis, paves the way for an increase in striker angle results in diminishing the deflection. Furthermore its impact results in the reduction of overall energy absorption (Nagel and Thambiratnam 2006). The percentage of the decrease was varied from 10% to 90% for various profiles. The beneficial effect in choosing the cross section which possesses high SEA for the application of crash tube was desirable. The hidden fact lies behind the higher values of SEA enables the thin-walled structure to be very light weight, but in contrary maximizing the energy absorption. The value of SEA was very essential during the phase of initial design it should absorb a significant amount of kinetic energy during the commencement of displacement of the crash tube during impact loading. Furthermore, the difference can be created between the energy absorption and deflection during impact loading.

To understand the deformation/failure mechanism of the thin-walled structures can be revealed by understanding the mechanism of energy absorption pattern. Interestingly in small velocity impact, the deformation mode was similar to be the case in quasi-static loading. On contrary in high-velocity impact inertia plays a crucial role in determining the deformation pattern changes and quasi-static SEA cannot be applicable in this case. The inclusion of strain rate effect contributes significant rise in yield stress for the corresponding energy absorption in the material. The occurred deflection (Fan *et al*. 2013) should be lesser in dynamic case par with the quasi-static loading.

A general remark observed in this study, which the average mean load (Faverage) decreases significantly with increase in impactor angle from 5° to 30°. The percentage reduction caused by incremental load angle pattern resulted in global bending due to the formation of plastic hinges in the structure.

The failure mechanism was the initiation of the transition phase from progressive crushing to overall global bending collapse. This feature was also observed in an earlier study (Han and Park 1999), where thin-walled collapse structure occurs in three phases, they were

(i) Initiation of progressive crushing (progressive zone)
(ii) Followed by progressive crushing to global bending (Transition zone)
(iii) The response occurred by global bending (Global Zone)

This study also emphasis on the impact of a different number of sides due to the occurrence of plastic hinges which causes local buckling. From Fig. 8, it is evident that octagon profile experiences global buckling during impact loading. A general remark may make here, considering all the profiles experiencing impact loading, the specimen possessing maximum thickness have higher resistance to the plastic bending due to higher stiffness. It enables the reduction of plastic hinges expressed in Fig. 17, experiencing in direct loading condition. In contrast, increase in thickness results in lower resistance and stiffness of the structure in case of oblique loading condition. This feature was also observed in a previous related study (Fan *et al*. 2013).

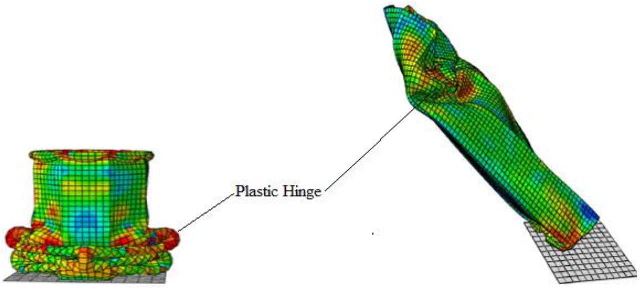

Fig. 17 Formation of plastic hinges during phase transition for hexagonal profiles

6. Conclusions

This paper examined the energy absorption and crash response of thin walled structures subjected to direct and oblique impact loading, using a validated FE model. The finite element method has been used to mitigate the insight of impact crash load response quantify the impact of peak load, mean load and hence energy absorption capacity of the thin-walled tubes for variations in geometric profile, load angle, wall thickness and initial length. The investigaion revealed that the circular thin-walled structures were found to be impressive energy absorbing device even though they can withstand oblique impact loading in par with direct loading with negligible minimum reduction energy absorption characteristics as the increasing load angle pattern. The design information and important findings can be outlined as follows.

- Changing the different cross-sectional profiles, consequently affects the energy-absorbing efficiency of the component with respect to the corresponding deformation.
- The significant reduction in energy absorption capacity is observed as the < 30° angle of applied load which increases for the given wall thickness irrespective of cross sections of the tube.
- It was found that the circular cross-sectional profile was a profound choice as better energy absorption application, taking into consideration of crash performance indicators. 2 mm thickness circular profile of perimeter 372 mm had energy absorption of 29.14 kJ and a CFE of 0.42 for direct loading and 32.57 kJ and 0.75 for oblique loading respectively. Furthermore, the circular profile exhibited higher SEA pattern as compared to other profiles both in direct and oblique loading.
- The average mean load (Faverage) decreases significantly when the impactor angle increases from 5° to 30° progressively. These percentage reductions

were due to the incremental load angle pattern, the results initiated the global bending due to the formation of plastic hinges in the structure. The failure mechanism was from the initiation of transition phase from progressive crushing to overall global bending collapse occurs in three phases,

(i) Initiation of progressive crushing (progressive zone)
(ii) Followed by progressive crushing to global bending (Transition zone)
(iii) The response occurred by global bending (Global Zone)

This study shown that the circular profile tubes appear to be advantageous in impact applications where direct and oblique impact load were expected. The generated information from the current research had its own merit and provokes guidance in design of thin walled structures of different cross sectional profiles enhancing the crashworthiness of vehicles experiencing oblique impact loading.

References

Abramowicz, W. and Jones, N. (1984a), "Dynamic axial crushing of sqaure tubes", *Int. J. Impact Eng.*, **2**(2), 179-208.

Abramowicz, W. and Jones, N. (1984b), "Dynamic axial crushing of circular tubes", *Int. J. Impact Eng.*, **2**(3), 263-281.

Abramowicz, W. and Weirzbicki, T. (1988), "Axial crushing of foam filled columns", *Int. J. Mech. Sci.*, **30**(3-4), 263-271.

Ahmad, Z. and Thambiratnam, D.P. (2009), "Dynamic computer simulation and energy absorption of foam filled conical tubes under axial impact loading", *Int. J. Comput. Struct.*, **87**(3-4), 186-197.

Alaghamdi, A. (2001), "Collapsible impact energy absorbers: an overview", *Thin-wall. Struct.*, **39**(2), 189-213.

Baaskaran, N., Ponappa, K. and Shankar, S. (2017), "Quasi-Static crushing and energy absorption characteristics of thin-walled cylinders with geometric discontinuities of various aspect ratios", *Latin Am. J. Solids Struct.*, **14**(9), 1767-1787.

Borvik, T., Hopperstad, O.S. and Reyes, M. (2003), "Empty and foam filled circular aluminium tubes subjected to axial and oblique quasistatic loading", *Int. J. Crashworth.*, **8**(5), 481-494.

Chung, S., Nurick, N. and Starke, R. (2008), "The energy absorption characteristics of double cell tubular profiles", *Thin-Wall. Struct.*, **5**(4), 289-317.

Duffy, J. (1979), "Testing techniques and material behavior at high rates of strain", *Int. J. Hardening*, **47**, 1-15.

Fan, Z., Lu, G. and Liu, K. (2013), "Quasistatic axial compression of thin walled tubes with different cross sectional shapes" , *Int. J. Eng. Struct.*, **55**, 80-89.

Fyllingen, O., Hopperstad, O.S. and Hanssen, G. (2010), "Modelling of tubes subjected to axial crushing", *Thin-Wall. Struct.*, **48**(2), 134-142.

Guillow, S.R., Lu, G. and Grzebieta, R.H. (2001), "Quasistatic axial compression of thin walled circular aluminium tubes", *Int. J. Mech. Sci.*, **43**(9), 2103-2123.

Han, D.C. and Park, S.H. (1999), "Collapse behavior of square thin walled columns subjected to oblique loads", *Thin-Wall. Struct.*, **35**(3), 167-184.

Hou, S.J., Li, S. and Long, Y. (2007), "Design optimization of regular hexagonal thin walled columns with crashworthiness criteria", *Int. J. Finite Elem. Anal. Des.*, **43**(6-7), 555-565.

Huang, M.Y., Tai, Y.S. and Hu, H. (2010), "Dynamic characteristics of high strength steel cylinders with elliptical geometric discontinuities", *Int. J. Theor. Appl. Fract. Mech.*, **54**(1), 44-53.

Jones, N. (1989), *Structural Impact*, Cambridge University Press, Cambridge, UK.

Karagiozova, D. and Jones, N. (2004), "Dynamic buckling of elastic plastic square tubes under axial impact-II: structural response", *Int. J. Impact Eng.*, **30**(2), 167-192.

Karbhari, V.M. and Chaoling, S. (2003), "Energy absorbing characteristics of circular frusta", *Int. J. Impact Eng.*, **8**, 471-479.

Krauss, C.A. and Laananen, D.H. (1994), "A parametric study of crush initiators for a thin walled tube", *Int. J. Vehicle Des.*, **15**(3-5), 384-401.

Langseth, M. and Hopperstad, O.S. (1996), "Static and dynamic axial crushing of square thin walled aluminium extrusions", *Int. J. Impact Eng.*, **18**(7-8), 949-968.

Langseth, M., Hopperstad, O.S. and Hanssen, A.G. (1998), "Crash behavior of thin walled aluminum members", *Thin-Wall. Struct.*, **32**(1-3), 127-150.

Mahdi, E. and Hamouda, A.M.S. (2012), "Energy absorption capability of composite hexagonal ring system", *Int. J. Mater. Des.*, **34**, 201-210.

Mamalis, A.G., Manolakos, G.A. and Demosthenous, G.A. (1991), "Axial plastic collapse of thin bimaterial tubes as energy dissipating systems", *Int. J. Impact Eng.*, **11**(2), 185-196.

Nagel, G.M. and Thambiratnam, D.P. (2005), "Computer simulation and energy absorption of tapered thin walled rectangular tubes", *Thin-Wall. Struct.*, **43**(8), 1225-1242.

Nagel, G.M. and Thambiratnam, D.P. (2006), "Dynamic simulation and energy absorption of tapered thin walled tubes under oblique impact loading", *Int. J. Impact Eng.*, **32**(10), 1595-1620.

Peixinho, N. and Pinho, A. (2007), "Study of viscoplasticity models for the impact behavior of high strength steels", *Transactions of ASME*, **2**(2), 114-123.

Qi, C., Yang, S. and Dong, F.L. (2012), "Crushing analysis and multi-objective crashworthiness optimization of tapered square tubes under oblique impact loading", *Thin-Wall. Struct.*, **59**, 103-119.

Reyes, A. and Langseth, M. (2002), "Crashworthiness of aluminium extrusions subjected to oblique loading: experiments and numerical analysis", *Int. J. Mech. Sci.*, **44**(9), 1965-1984.

Santosa, S.P., Wierzbicki, T., Hanssen, A.G. and Langseth, M. (2000), "Experimental and numerical studies of foam filled sections", *Int. J. Impact Eng.*, **24**(5), 509-534.

Tai, Y.S., Huang, M.Y. and Hu, H.T. (2010), "Axial compression and energy absorption characteristics of high strength thin walled cylinders under impact load", *Int. J. Theore. Appl. Fract. Mech.*, **53**, 1-8.

Tarlochan, F. and Samer, F. (2013), "Design of thin walled structures for energy absorption applications: Design for crash injuries mitigation using magnesium alloy", *Int. J. Res. Eng.*, **19**, 2321-2329.

Tarlochan, F., Samer, F., Hamouda, A.M.S., Ramesh, S. and Khalid, K. (2013), "Design of thin walled structures for energy absorption applications: Enhancement of crashworthiness due to axial and oblique impact forces", *Thin-Wall. Struct.*, **71**, 7-17.

Thornton, P.H., Mahmood, H.F. and Magee, C.L. (1983), "Energy absorption of structural collapse", *Structural Crashworthiness, Butterworths*, London, England.

Vahdatazad, N. and Ebrahimi, S. (2016), "Energy absorption characteristics of diamond core columns under axial crushing loads", *Steel Compos. Struct., Int. J.*, **21**(3), 605-628.

Vinayagar, K. and Kumar, A.S. (2017), "Multi-response optimization of crashworthiness parameters of bi-tubular structures",

Steel Compos. Struct., Int. J., **23**(1), 31-40.
Witteman, W.J. (1999), "Improved Vehicle crashworthiness design by control of the energy absorption for different collision situation", Thesis; Eindhoven University of Technology, Netherlands, 41 p.
Yu, H., Gu, Y. and Lai, X. (2009), "Rate dependent behavior and constitutive model of DP600 steel at strain rate from 10-4 to 103s-1", *Int. J. Mater. Des.*, **30**(7), 2501-2505.

BU